

## Review Article

Li Fu<sup>#</sup>, Xiaozhu Liu<sup>#</sup>, Junyi Cao<sup>#</sup>, Huan Li, Anyou Xie, and Yue Liu\*

# Recent advance in electrochemical immunosensors for lung cancer biomarkers sensing

<https://doi.org/10.1515/revac-2023-0068>

received August 29, 2023; accepted November 15, 2023

**Abstract:** Lung cancer has a high mortality rate largely due to late-stage diagnosis. Detecting protein and genetic biomarkers through electrochemical immunosensors enables non-invasive early diagnosis. This review discusses recent advances in electrochemical immunosensors for detecting clinically relevant lung cancer biomarkers. The use of nanomaterials like graphene, carbon nanotubes, metal nanoparticles, and conducting polymers in sensor fabrication improves electron transfer kinetics, enhances signal transduction, and allows higher antibody loading. Smart surface immobilization strategies optimize antibody orientation and binding capacity. Amplification approaches utilizing nanomaterials, enzymes, polymers, dendrimers, and DNA nanostructures are applied to enhance output signal per binding event. Various electroanalytical techniques including amperometry, potentiometry, impedance spectroscopy, and voltammetry are employed for quantitative monitoring. Recent immunosensors showcase low detection limits and wide linear ranges for measurement of

major biomarkers like carcinoembryonic antigen, neuron specific enolase, and cytokeratin fragment 21-1. Emerging biomarkers such as microRNAs and circulating tumor cells have also been targeted. However, reproducibility, selectivity, multiplexing, and integration with point-of-care platforms need improvement for widespread clinical translation. Overall, electrochemical immunosensors hold immense potential for sensitive, affordable lung cancer diagnosis if ongoing efforts can address current limitations.

**Keywords:** lung cancer, biomarkers, immunosensors, nanomaterials, electrochemistry

## 1 Introduction

Lung cancer remains one of the most commonly diagnosed cancers and the leading cause of cancer mortality worldwide. It arises from the uncontrolled growth of abnormal cells in the lung tissue, usually originating in the epithelial cells lining the airways [1–3]. Lung cancer is clinically divided into two main types – small cell lung cancer which accounts for 15% of cases, and the more prevalent non-small cell lung cancer (NSCLC) representing 85% of cases [4–6]. Despite advances in treatment modalities, the prognosis for lung cancer patients remains poor, with a 5-year survival rate of only 18% [7]. This high mortality rate is largely attributed to late-stage diagnosis, as patients tend to be asymptomatic in early stages [8]. Hence, there is an urgent need for diagnostic techniques that can detect lung cancer at an early stage when it is still localized and potentially curable.

The analysis of biomarkers present in body fluids offers a very promising non-invasive approach for early lung cancer diagnosis and screening. Lung cancer biomarkers refer to measurable indicators of disease onset and progression that can be detected and quantified using bio-sensor devices [9]. A number of protein and genetic biomarkers have been identified, including carcinoembryonic antigen (CEA) [10], neuron specific enolase (NSE) [11],

<sup>#</sup> These authors contributed equally.

**\* Corresponding author:** Yue Liu, Department of Pediatrics, First People's Hospital of Zigong City, Zigong, 643000 China, e-mail: 2528049970@qq.com

**Li Fu:** Key Laboratory of Novel Materials for Sensor of Zhejiang Province, College of Materials and Environmental Engineering, Hangzhou Dianzi University, Hangzhou, 310018 China, e-mail: lifu.ac@gmail.com, fuli@hdu.edu.cn

**Xiaozhu Liu:** Department of Critical Care Medicine, Beijing Shijitan Hospital, Capital Medical University, Beijing, 100038 China

**Junyi Cao:** Department of Medical Quality Control, First People's Hospital of Zigong City, Zigong, 643000 China

**Huan Li:** Chongqing College of Electronic Engineering, Chongqing, 401331 China

**Anyou Xie:** Key Laboratory of Novel Materials for Sensor of Zhejiang Province, College of Materials and Environmental Engineering, Hangzhou Dianzi University, Hangzhou, 310018 China

cytokeratin fragment 21-1 (CYFRA21-1) [12], microRNA-21 (miR-21) [13], cell-free DNA [14], and circulating tumor cells [15]. The development of rapid, inexpensive, and ultrasensitive biosensors capable of detecting such biomarkers, even at low concentrations in body fluids, can enable early diagnosis which is key to improving clinical outcomes through timely therapeutic intervention [16,17].

Table 1 shows the common methods and features of different analytical methods for lung cancer biomarkers detection. It can be seen that electrochemical immunosensors offer high sensitivity down to the  $\text{pg}\cdot\text{mL}^{-1}$  or even  $\text{fg}\cdot\text{mL}^{-1}$  range for lung cancer biomarker detection due to signal amplification strategies. However, they face challenges related to reproducibility, selectivity, and integration into point-of-care devices. ELISA assays have high selectivity but are more complex, time-consuming, and costly. qPCR provides the highest sensitivity but requires specialized equipment and reagents. Mass spectrometry also achieves very low detection limits but is expensive and complex [18].

The performance of electrochemical immunosensors relies heavily on the choice of electrode materials and nanocomposites [19]. Carbon-based nanomaterials such as graphene and carbon nanotubes (CNTs) offer high conductivity, surface area, and biocompatibility [20]. Metal and metal oxide nanoparticles (NPs) like gold (Au), silver (Ag), and iron oxide can enhance electron transfer kinetics and immobilize capture biomolecules [21]. Conducting polymers further improve electrical properties. Additionally, hybrid nanocomposites synergistically combine the advantages of multiple materials for optimized immunosensor response.

Various immobilization strategies are utilized to attach capture biomolecules such as antibodies onto the electrode surface with optimal orientation and high binding capacity [22]. Common approaches include physical adsorption, covalent binding, affinity-based binding, and electrostatic interaction. Once immobilized, the antibody specifically binds to the target antigen, but the generated signal needs to be amplified for improved detection sensitivity. Signal

enhancement strategies include use of enzymes, NPs, conducting polymers, dendrimers, and DNA nanostructures [23].

A range of electrochemical techniques are leveraged for transduction of the binding event into a measurable analytical signal. These include amperometry, potentiometry, impedance spectroscopy, and voltammetry. Together, the advances in nanomaterials, immobilization strategies, signal amplification, and electrochemical detection techniques have enabled unprecedented performance in electrochemical immunosensors for detecting clinically relevant lung cancer biomarkers like CEA, NSE, and CYFRA21-1 even at extremely low concentrations [24]. This review discusses recent advances in electrochemical immunosensors for detecting lung cancer biomarkers, focusing on key aspects like nanomaterials, immobilization strategies, signal enhancement approaches, and detection techniques. The use of novel nanocomposites and conductive polymers has enabled the development of immunosensors with enhanced sensitivity, stability, and reproducibility. Smart surface immobilization methods allow optimal antibody orientation and binding capacity. Amplification strategies involve nanomaterials, enzymes, polymers, dendrimers, and DNA nanostructures that amplify signal response. Various electroanalytical techniques are leveraged for quantitative monitoring of biomarker binding events. Recent applications showcase low detection limits and wide linear ranges for measurement of major protein and genetic lung cancer biomarkers. However, realization of their full clinical potential requires addressing limitations related to reproducibility, selectivity, multiplexing, and integration with point-of-care platforms.

## 2 Electrode materials and nanocomposites

The performance of electrochemical immunosensors relies heavily on the choice of electrode materials and

**Table 1:** Comparison of different methods for lung cancer biomarker detection

Method	Common detection limit	Advantages	Disadvantages
Electrochemical immunosensors	$0.1 \text{ pg}\cdot\text{mL}^{-1}$	High sensitivity, low cost, portability	Reproducibility issues, selectivity challenges
ELISA	$1 \text{ ng}\cdot\text{mL}^{-1}$	Well established, high selectivity	Complex procedure, high cost, time consuming
qPCR	$1 \text{ fM}$	High sensitivity, specificity	Requires specialized equipment and reagents, complex workflow, high cost
Mass spectrometry	$0.1 \text{ pg}\cdot\text{mL}^{-1}$	High sensitivity, specificity	Complex sample preparation, requires specialized equipment, high cost

nanocomposites used. The electrode material provides the transduction interface where the biomarker binding event is translated into a measurable electrical signal. Nanomaterials offer several advantages like high surface area, conductivity, biocompatibility, and catalytic properties that enhance sensor response.

## 2.1 Carbon-based nanomaterials

Carbon nanomaterials such as graphene, CNTs, and biochar have become very popular for electrochemical immunosensor fabrication owing to their exceptional electrical, mechanical, and chemical properties. Graphene is a 2D sheet of  $sp^2$  hybridized carbon atoms arranged in a honeycomb lattice. It has very high specific surface area, excellent conductivity, good mechanical strength and flexibility, ease of functionalization, and biocompatibility. Graphene can be synthesized via chemical vapor deposition or solution-based oxidation-reduction methods to produce graphene oxide which is then reduced. Graphene promotes electron transfer kinetics and provides a suitable microenvironment for immobilizing biomolecules. For example, Chen et al. [25] developed an electrochemical immunosensor for sensitive detection of CEA. Graphene was used as the sensing material due to its excellent properties such as large surface area, high electrical conductivity and good biocompatibility. The researchers functionalized carboxyl graphene nanosheets with toluidine blue to form CGS-TB nanocomposites (Figure 1a). Toluidine blue acted as an electrochemical mediator to enhance the sensing signal. The CGS-TB nanocomposites were then conjugated with anti-CEA antibodies to form CGS-TB-Ab bioconjugates. These bioconjugates acted as signal tags for detecting CEA. Chitosan-AuNPs were used as the sensing platform. They were immobilized on the electrode surface and the capture anti-CEA antibodies were attached. This allowed the capture antibodies to capture CEA antigens from the sample

solution. In the immunosensor, the CGS-TB-Ab bioconjugates bound to the captured CEA antigens, forming a sandwich immunoassay. The toluidine blue molecules on the graphene nanosheets generated an electrochemical signal that was proportional to the CEA concentration.

Carbon nanotubes are 1D hollow tubular structures made of rolled up graphene sheets. They have very high tensile strength, surface area, and electrical conductivity. Single-walled CNTs and multi-walled CNTs are commonly used. CNTs can be functionalized to attach capture biomolecules. The high conductivity of CNTs enhances electron transfer and signal transduction. For example, Xu et al. [26] focused on developing a label-free electrochemical immune microelectrode array for the sensitive detection of CEA. The researchers successfully synthesized a chitosan-multi-walled carbon nanotube-thionine (CS-MWCNTs-THI) hybrid film through a one-step electrochemical deposition process. This hybrid film was then employed to immobilize anti-CEA antibodies, enabling the fabrication of a simple and highly sensitive immune microelectrode array (MEA). The detection mechanism was based on the formation of antigen-antibody immunocomplexes leading to decreased response currents, with the reduction directly proportional to CEA concentration. The immune MEA exhibited a wide linear range for CEA detection ( $1 \text{ pg}\cdot\text{mL}^{-1}$  to  $100 \text{ ng}\cdot\text{mL}^{-1}$ ) and a low limit of detection ( $0.5 \text{ pg}\cdot\text{mL}^{-1}$  with signal noise ratio = 3). The hybrid film's nano-porous structure and the synergistic effect of MWCNTs and THI contributed to the enhanced electrochemical performance.

Both graphene and CNTs facilitate electrochemical biomarker sensing with lower overpotentials, higher sensitivity, and lower detection limits compared to traditional electrode materials. However, graphene offers better mechanical stability and ease of surface modification compared to CNTs which tend to aggregate. Combining graphene and carbon nanotubes is also a strategy. Gu et al. [27] developed an innovative electrochemical immunosensor for the detection of CA125. The sensor, composed of nitrogen-doped reduced

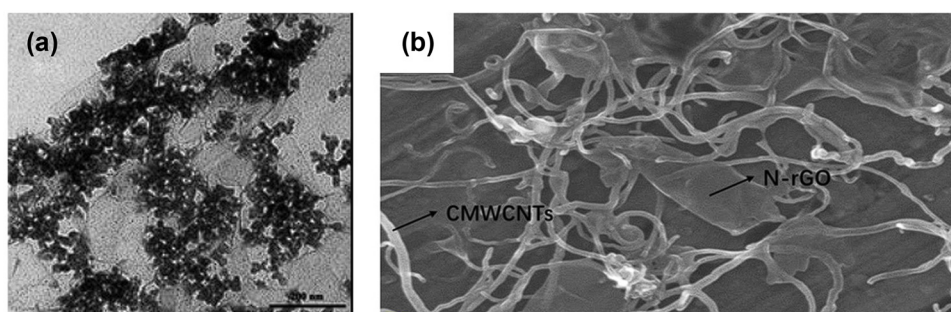


**Figure 1:** (a) TEM image of CGS-TB nanocomposites. (b) SEM image of N-rGO@CMWCNTs/CS@AuNPs. Reproduced with permission from refs. [25,27].

graphene oxide (N-rGO), carboxylated MWCNTs (CMWCNTs), CS, and AuNPs on a glassy carbon electrode (GCE) (Figure 1b), exhibited exceptional sensitivity and specificity. Through careful optimization, the sensor achieved a wide linear detection range spanning from  $0.1 \text{ pg}\cdot\text{mL}^{-1}$  to  $100 \text{ ng}\cdot\text{mL}^{-1}$  of CA125, with a low detection limit of  $0.04 \text{ pg}\cdot\text{mL}^{-1}$ . Notably, the immunosensor showcased robust reproducibility, stability, and selectivity, demonstrating its potential for clinical applications. The sensor's effectiveness was validated by successful analysis of spiked serum samples and real serum samples from lung cancer patients, with recovery experiments yielding accurate results and minimal variability.

Biochar is an excellent carbon material for the design of electrochemical immunosensors. Biochar is a porous carbon material produced from the pyrolysis of biomass waste such as wood, agricultural residues, and manure. It has a high surface area, stable structure, good electrical conductivity, and abundant surface functional groups. These properties make biochar very suitable for use as an electrode material in electrochemical immunosensors [28–30]. For example, Cancelliere et al. [31] presented a new electrochemical immunosensor based on screen-printed electrodes modified with biochar for the sensitive detection of interleukin-6 (IL-6). The use of biochar, produced from brewers' spent grain, provides both an electrochemical enhancement of the electrode's electron transfer kinetics and a protein binding substrate for antibody immobilization. Two IL-6 immunosensors were fabricated using different IL-6 antibodies. The layer-by-layer assembly of the immunosensors was characterized electrochemically and optimized. The biochar-modified electrodes showed improved conductivity compared to bare electrodes. The immunosensors demonstrated good analytical performance in buffer and human serum, with limits of detection as low as  $4.8 \text{ pg}\cdot\text{mL}^{-1}$ , linear ranges from 26 to  $138 \text{ pg}\cdot\text{mL}^{-1}$ , and recoveries from 82% to 95%. They also showed selectivity for IL-6 over other cytokines and stability for up to 14 days of storage.

## 2.2 Metal NPs

Metal NPs made from Au, Ag, platinum (Pt), etc., have great potential for electrochemical immunosensor applications because of their high conductivity, biocompatibility, catalytic properties, and high surface-to-volume ratio.

AuNPs are the most widely used. AuNPs can be synthesized in different shapes and sizes and are stable, non-toxic, and easily functionalized. AuNPs can adsorb proteins without altering their biological activity. Furthermore, AuNPs enhance the immobilization of capture antibodies and act as electrochemical

labels when functionalized with secondary antibodies or enzymes for signal amplification. For example, Hu et al. [32] aimed to develop a biosynthesis method for AuNPs using an extract from *Eucalyptus leaves*. The synthesized AuNPs demonstrated significant potential as a natural antioxidant, displaying excellent free radical scavenging activity. The NPs were found to be roughly spherical in shape with sizes ranging from 10 to 30 nm. The biosynthesized AuNPs exhibited strong antioxidant activity, outperforming the standard ascorbic acid antioxidant in a DPPH assay with an IC<sub>50</sub> value of  $7.25 \mu\text{g}\cdot\text{mL}^{-1}$ . Additionally, the AuNPs demonstrated notable antibacterial effects against several pathogenic bacterial strains. The results highlight the potential of Eucalyptus leaf extract-synthesized AuNPs for their application in the biomedical and pharmaceutical fields due to their antioxidant and antibacterial properties. Nguyen and Jen [33] reported a novel microfluidic chip designed to capture A549 human lung adenocarcinoma cells by utilizing a self-assembled monolayer (SAM) of AuNPs functionalized with cell-specific aptamers. The chip's fabrication involves creating a SAM area on a glass substrate using photolithography and AuNP attachment through aminosilane treatment. Thiol-labeled aptamers are then self-assembled onto the AuNP layer. The success of this modification is confirmed through electrical impedance spectroscopy (EIS), showing enhanced impedance responses with the presence of the SAM of AuNPs. Our previous publication also used a glucose oxidase-functionalized gold nanorod probe that can catalyze the deposition of AuNPs [34]. An immunosensor was constructed by immobilizing capture antibodies on a carbon nanotube-modified screen-printed carbon electrode (SPCE). After the sandwich immunoassay, the gold nanorod probe is captured on the immunosensor surface. Then, the glucose oxidase catalyzes the deposition of AuNPs from a developer solution containing glucose, mediator, and gold salt. The electrochemical stripping analysis of both the gold nanorods and AuNPs produces an amplified signal response, resulting in ultrahigh sensitivity (Figure 2). When detecting CEA as a model analyte, the method achieved an excellent performance. It had a wide linear detection range from  $0.01$  to  $100 \text{ ng}\cdot\text{mL}^{-1}$  with a detection limit as low as  $4.2 \text{ pg}\cdot\text{mL}^{-1}$ .

AgNPs have high electrical conductivity and exhibit electrocatalytic activity towards hydrogen peroxide, allowing their use in enzyme-based amperometric sensors. AgNPs can also bind amino groups in proteins through Ag-NH<sub>2</sub> linkage. Asadzadeh-Firouzabadi and Zare [35] focused on developing an electrochemical nanogenosensor for the sensitive detection of miR-25 using AgNPs/single-walled carbon nanotubes (SWCNTs) nanohybrid as an electroactive label. The nanohybrid was characterized through TEM and electrochemical methods, revealing successful decoration of AgNPs on SWCNT

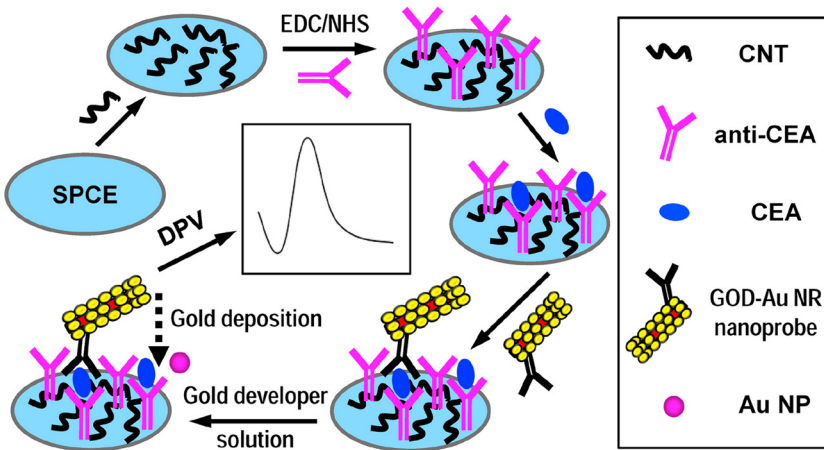


**Figure 2:** Schematic of sandwich immunoassay based on the signal tracing of the glucose oxidase-functionalized nanoprobe. Reproduced with permission from ref. [34].

surfaces. The nanosensor's preparation steps were monitored using cyclic voltammetry and electrochemical impedance spectroscopy, confirming the immobilization of the probe and subsequent hybridization with miR-25. The nanogenosensor demonstrated excellent selectivity and sensitivity, successfully distinguishing between complementary, one-base mismatch, and non-complementary targets. The sensor exhibited a linear range for miR-25 concentration from 1 pM to 0.1 nM, with a detection limit of 0.313 pM. Moreover, the nanogenosensor's reliability was confirmed by analyzing miR-25 in human plasma samples through spiking experiments, showcasing recovery rates between 97.58% and 105.91% with a low relative standard deviation. Jafari-Kashi et al. [36] reported a novel electrochemical DNA biosensor designed to detect the lung cancer biomarker CYFRA21-1. The biosensor, constructed on a modified glassy carbon electrode with layers of rGO, PPy, and AgNPs, achieves remarkable sensitivity and selectivity. Through systematic optimization of experimental conditions, the biosensor demonstrates a wide linear detection range (10 fM to 1  $\mu$ M) and a low detection limit (2.4 fM). The use of AgNPs serves to enhance the biosensor's performance, contributing to its excellent reproducibility and enabling the specific recognition of the target biomarker.

PtNPs similarly enhance electron transfer kinetics and increase the sensor sensitivity. The high surface area and biocompatibility of metal NPs ultimately allow more target analyte binding and improved detection limits. For example, Lv et al. [37] described the development of a highly sensitive electrochemical immunoassay for the detection of the lung cancer biomarker CYFRA21-1. The sensor utilizes a conjugated nanosheet called TPAPCN that exhibits aggregation-induced electrochemiluminescence (AIECL) as the signal label. When aggregated, TPAPCN produces a much stronger

ECL emission signal compared to when dispersed. PtNPs were synthesized on the TPAPCN nanosheets to improve electron transfer and boost the ECL signal. The TPAPCN was conjugated to a signal antibody. In addition, three-dimensional graphene decorated with PtNPs and the electroactive molecule THI (3D-GN/PtNPs/Th) was used to immobilize the capture antibody and provide a stable internal electrochemical signal. By measuring the ratio of the ECL signal from the TPAPCN label and the electrochemical signal from the THI, the immunosensor eliminates noise and interference, improving detection accuracy. The sensor exhibited excellent sensitivity with a wide linear detection range of 50  $\text{fg}\cdot\text{mL}^{-1}$  to 1  $\text{ng}\cdot\text{mL}^{-1}$  and a low limit of detection of 16  $\text{fg}\cdot\text{mL}^{-1}$  for CYFRA21-1.

## 2.3 Metal oxides

Metal oxides including iron oxide ( $\text{Fe}_3\text{O}_4$ ), titanium oxide ( $\text{TiO}_2$ ), zinc oxide ( $\text{ZnO}$ ), copper oxide ( $\text{CuO}$ ), etc., have also been incorporated into immunosensor electrode materials. They offer biocompatibility, high stability, and good electrocatalytic behavior.

$\text{Fe}_3\text{O}_4$  NPs in particular improve electron transfer and amplification of signal response. Wang et al. [38] described the development of a sensitive electrochemical immunoassay for detecting CEA levels. The immunosensor used a sandwich technique, with the antibody immobilized on the surface and magnetic  $\text{Ag}/\text{MoS}_2@\text{Fe}_3\text{O}_4$  NPs used as a label. The  $\text{Fe}_3\text{O}_4$  in the NPs allows them to be firmly attached to the electrode surface due to its magnetic properties, avoiding loss of the label. Using differential pulse voltammetry, the

immunosensor was able to detect CEA in the range of 0.0001 to 20 ng·mL<sup>-1</sup>, with a low detection limit of 0.03 pg·mL<sup>-1</sup>. The immunosensor also demonstrated excellent stability, selectivity, and reproducibility. The use of the magnetic Fe<sub>3</sub>O<sub>4</sub> NPs was key to the sensitive detection and performance of the immunosensor by keeping the label immobilized on the electrode surface.

TiO<sub>2</sub> NPs have been used to enhance antibody immobilization and to develop enzyme-linked immunoassays. Mavrič *et al.* [39] provided an overview of electrochemical biosensors based on TiO<sub>2</sub> nanomaterials for early detection of cancer biomarkers. TiO<sub>2</sub> nanostructures like nanotubes, NPs, and nanowires can enhance sensitivity by increasing surface area for binding events. Important characteristics for biosensing are high surface area, appropriate surface chemistry for biomolecule attachment, and efficient electron transfer, which can be tuned in TiO<sub>2</sub> by creating oxygen vacancies and Ti<sup>3+</sup> defects. Sensors are often designed with additional nanomaterials like AuNPs, graphene, or semiconductor quantum dots to amplify signals and improve electron transfer. Reported detection limits are very low, down to the fg·mL<sup>-1</sup> range for some protein biomarkers, showing high sensitivity.

ZnO NPs and CeO<sub>2</sub> NPs also display strong protein adsorption ability to enable detection of biomarkers. For example, Che *et al.* [40] reported the development of an electrochemical sensor using ZnO/porous graphene oxide (ZnO/HGO) nanocomposites for the detection of the lung cancer biomarkers CEA and CA153. The ZnO NPs were grown on HGO sheets using a hydrothermal method. The ZnO/HGO composite was used to modify a glassy carbon electrode. Antibodies for CEA and CA153 were then immobilized on the electrode surface to enable specific binding to the target antigens. The sensor showed good linearity for CEA detection from 0.1–20 ng·mL<sup>-1</sup> with a detection limit of 0.07 ng·mL<sup>-1</sup>. For CA153, the linear range was 0.5–70 U·mL<sup>-1</sup> and the detection limit was 0.22 U·mL<sup>-1</sup>. The ZnO NPs provided good biocompatibility and a high surface area, while the HGO increased material transport and active sites. Yu *et al.* [41] described the development of an electrochemical immunosensor for detecting the biomarker NSE. The immunosensor uses a sandwich structure with antibodies and nanocomposite materials to amplify the detection signal. A key component is the use of Au/Cu<sub>x</sub>O@CeO<sub>2</sub> nanocomposites as a label material. CeO<sub>2</sub> NPs were deposited onto Cu<sub>x</sub>O nanocubes along with AuNPs to form a spiny surface. CeO<sub>2</sub> helped provide favorable catalytic activity and stability when combined with Cu<sub>x</sub>O. The rough nanocomposite surface increased surface area to carry more antibodies. When tested, the immunosensor showed high sensitivity with a detection limit of 31.3 fg·mL<sup>-1</sup>, a wide linear range of 50

fg·mL<sup>-1</sup> to 100 ng·mL<sup>-1</sup>, and good performance in selectivity and stability. The inclusion of CeO<sub>2</sub> in the nanocomposite label helped enhance catalytic activity and signal amplification in the sensor.

## 2.4 Conducting polymers

Conducting polymers such as polyaniline (PANI), polypyrrole (PPy), and poly(3,4-ethylenedioxythiophene) (PEDOT) have also garnered interest for fabricating immunosensor electrodes owing to their electrical conductivity, biocompatibility, environmental stability, and ease of synthesis. These polymers can be chemically or electrochemically polymerized to form uniform thin films on electrode surfaces. Their conductive backbone facilitates electron transfer, while their side chains can be modified with functional groups for covalent antibody immobilization. Conducting polymers enhance surface area, improve electrochemical reactivity, and lower electrochemical impedance.

For example, PANI with good biocompatibility and electrical conductivity has been widely employed. The amine groups on PANI enable covalent binding of antibodies. PANI also helps maintain biological activity of immobilized antibodies. Park *et al.* [42] demonstrated an electrochemical aptasensor using a PANI/CNT nanocomposite for detecting vascular endothelial growth factor (VEGF165). The nanocomposite was synthesized by polymerizing aniline on the surface of acid-treated CNTs. Adding PANI to the CNTs increased the sensor's sensitivity and stability compared to CNTs alone, due to PANI's high conductivity and large surface area. The VEGF165 aptamer was covalently attached to the PANI/CNT surface (Figure 3). The sensor detected VEGF165 with high sensitivity from 0.5 pg·mL<sup>-1</sup> to 1 µg·mL<sup>-1</sup>, with a detection limit of 0.4 pg·mL<sup>-1</sup>. This is better performance than other reported VEGF sensors. The sensor also showed good selectivity for VEGF165 against other proteins. The use of the PANI/CNT nanocomposite and aptamer binding provided excellent sensitivity and selectivity for detecting the VEGF165 biomarker.

Similarly, PPy provides a biocompatible microenvironment to maintain antibody binding activity. Kivrak *et al.* [43] described the development of an electrochemical aptasensor using PPy nanofibers for the detection of NSCLC cells. The aptasensor uses a pencil graphite electrode modified with composite nanofibers made of polyacrylonitrile (PAN) and 10% PPy by weight. The high conductivity and porosity of PPy enhances the performance of the nanofiber-modified electrode. The aptamer specific to the target A549 cancer cells is immobilized on the surface. When the

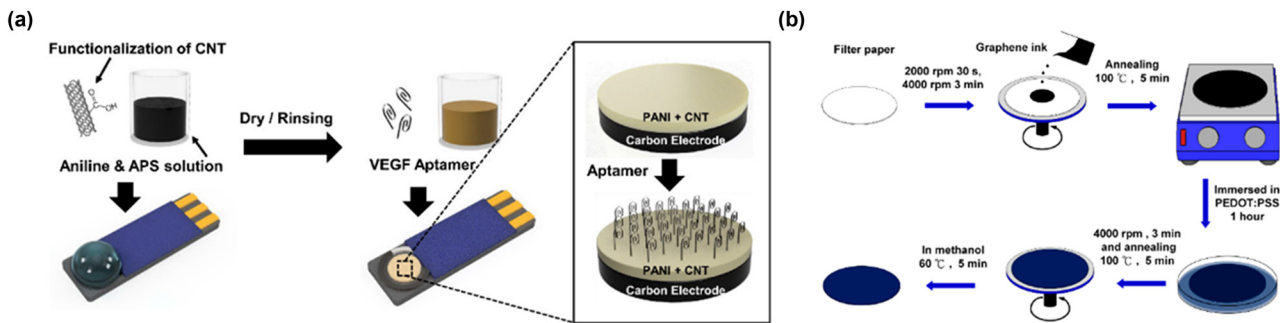


**Figure 3:** (a) Schematic illustration of the preparation of the PANI/CNT nanocomposite and the assembled VEGF165 aptamer on the sensor surfaces for the VEGF sensors. (b) Fabrication and modification process of graphene-PEDOT:PSS modified paper-based aptasensor. Reproduced with permission from refs. [42,44].

target cells bind to the aptamer, it causes an increase in charge transfer resistance measured by electrochemical impedance spectroscopy. The aptasensor shows high sensitivity and selectivity for detecting A549 cells down to  $1.2 \times 10^3$  cells·mL $^{-1}$ , with human cervical cancer HeLa cells used as a negative control. The PPy-containing nanofiber electrode interface enables sensitive impedimetric detection of the aptamer-cancer cell interactions.

Copolymers combining PSS and PEDOT have also been synthesized to further improve electrochemical properties and leverage synergistic effects. The high surface area and permeability, good electrical conductivity, and biocompatibility of conducting polymers ultimately result in higher loading of capture antibodies and lower detection limits. Yen et al. [44] described the development of a low-cost paper-based electrochemical aptasensor for detecting CEA. The sensor uses a graphene and PEDOT:PSS nanocomposite coating on paper to create a conductive and sensitive substrate for aptamer immobilization. Modifying the paper with PEDOT:PSS helped improve the conductivity and sensing performance of the electrode. The aptasensor showed a good linear detection range of 0.77–14 ng·mL $^{-1}$  for CEA and a limit of detection around 1 ng·mL $^{-1}$  in serum samples. The key benefit of PEDOT:PSS modification was enhancing the conductivity and sensitivity of the paper-based electrode in a cost-effective and accessible way.

### 3 Immobilization strategies

The performance of electrochemical immunosensors depends significantly on the immobilization strategy utilized to attach the capture biomolecules onto the electrode surface. The objective is to achieve high loading capacity, optimal orientation, strong binding affinity, and minimal non-specific adsorption [45]. Commonly used immobilization approaches include

physical adsorption, covalent binding, affinity-based attachment, and electrostatic interaction.

Physical adsorption involves non-covalent immobilization based on weak interactions such as van der Waals, hydrogen bonding, and hydrophobic interactions between the capture biomolecules and electrode surface. It is the simplest technique and preserves the bioactivity of antibodies or aptamers since it does not involve harsh chemical treatment. For example, the van der Waals interaction plays an important role in allowing the MoS<sub>2</sub> nanosheets to be stably dispersed in an aqueous solution by the flavin mononucleotide sodium salt (FMNs) [46]. Specifically, bulk MoS<sub>2</sub> was exfoliated into nanosheets via ultrasonication. However, the MoS<sub>2</sub> nanosheets are hydrophobic and tend to agglomerate in water due to lack of hydrophilic groups. FMNs contain an aromatic, conjugated structure that can adsorb onto the basal plane of the MoS<sub>2</sub> nanosheets via van der Waals interactions. The adsorbed FMNs provides hydrophilicity and steric hindrance that stabilizes the dispersion of the MoS<sub>2</sub> nanosheets in water. The FMNs/MoS<sub>2</sub> nanocomposite showed excellent electrochemical properties when immobilized on an electrode, likely due to the high conductivity and large surface area of the MoS<sub>2</sub> nanosheets. The phosphonate groups on the FMNs allowed covalent immobilization of DNA probes for detection of target DNA. Hydrogen bonding between polyethylene glycol (PEG) and the antibodies plays an important role in the electrochemical immunosensor [47]. PEG helps immobilize the antibodies onto the SPCE surface (Figure 4). The paper mentions that PEG can form multiple hydrogen bonds with the amino acid residues and main chain NH groups of the antibodies. This allows more antibodies to attach to the PEG-modified SPCE surface. PEG helps stabilize the binding sites (paratopes) of the immobilized antibodies. The hydrogen bonding between PEG and the antibodies likely preserves the structure of the antibody binding sites. This allows the antibodies to retain their specificity and binding affinity for the target

antigen. The preserved antibody binding sites lead to better immunorecognition of the target antigen (ENO1) and subsequent binding of the detection antibodies tagged with AuNPs. This results in a stronger electrochemical signal in the sensor. Comparisons showed that the PEG-modified SPCE immobilized fewer antibodies than the bare SPCE, but the PEG-modified sensor gave much higher signals. This suggests that the PEG layer helped maintain more functional and properly folded antibodies on the surface.

However, physically adsorbed biomolecules are randomly oriented and lack stability. They are prone to leaching and denaturation, which reduces shelf-life. Graphene, CNTs, AuNPs, and polymers like chitosan are commonly used to physically adsorb capture antibodies via hydrophobic and  $\pi$ - $\pi$  stacking interactions [48–51]. For example,  $\pi$ - $\pi$  stacking interactions help immobilize the ssDNA on the graphene quantum dots-ionic liquid-nafion (GQDs-IL-NF) composite film modified electrode [52]. The GQDs have  $\pi$  electrons that can interact with the aromatic nucleic acid bases of ssDNA through  $\pi$ - $\pi$  stacking. This allows the capture of the methylene blue-labeled ssDNA substrates on the electrode surface. It enables differentiation between ssDNA and dsDNA. The GQDs can interact with ssDNA via  $\pi$ - $\pi$  stacking but not the more rigid dsDNA structure. This is utilized when the auxiliary DNA hybridizes with the methylene blue-labeled substrate DNA to form dsDNA, which detaches from the GQDs surface leading to a drop in signal. It contributes to the high sensitivity of the aptasensor. The strong  $\pi$ - $\pi$  interaction facilitates binding of large amounts of the methylene blue-labeled ssDNA substrates to the GQDs surface after the target-induced DNAzyme recycling amplification. This gives a

high electrochemical signal for sensitive detection of the target protein. While easy to implement, the weak binding limits sensor reproducibility and makes this approach unsuitable for long-term monitoring applications.

Covalent binding forms strong and stable covalent linkage between the capture element and nanomaterial electrode surface, conferring high stability. A range of functional groups can be used for covalent crosslinking such as amine, carboxyl, aldehyde, hydroxyl, sulfhydryl, etc. [53,54]. For example, covalent bonding was used to immobilize the antibodies onto the signal tags (Au-pThi and Au-pMCP) [55]. The authors first activated the antibodies using 1-ethyl-3-(3-dimethylaminopropyl)carbodiimide (EDC)/n-hydroxysuccinimide (NHS) to form amine-reactive NHS esters. Then, the activated antibodies were covalently bonded to the Au-pThi and Au-pMCP nanocomposites. This allows the antibodies to be stably linked to the signal tags. In another work [56], a sensor used gold interdigitated electrode arrays modified with IL-6 antibodies, which was covalently bound through a carboxylic acid group. This covalent binding ensured that the antibodies were stably immobilized on the electrode surface. The sensor detected IL-6 by measuring changes in the current when a redox probe, ferrocyanide/ferricyanide, interacted with the electrode.

Gold screen-printed electrodes offer a convenient platform for electrochemical immunoassays. Materials such as MWCNTs with carboxylic acid functional groups and biochar can be modified on the gold screen-printed electrode surface via covalent immobilization. This can be achieved using carbodiimide-mediated amide coupling reactions to form covalent linkages between the amine groups of

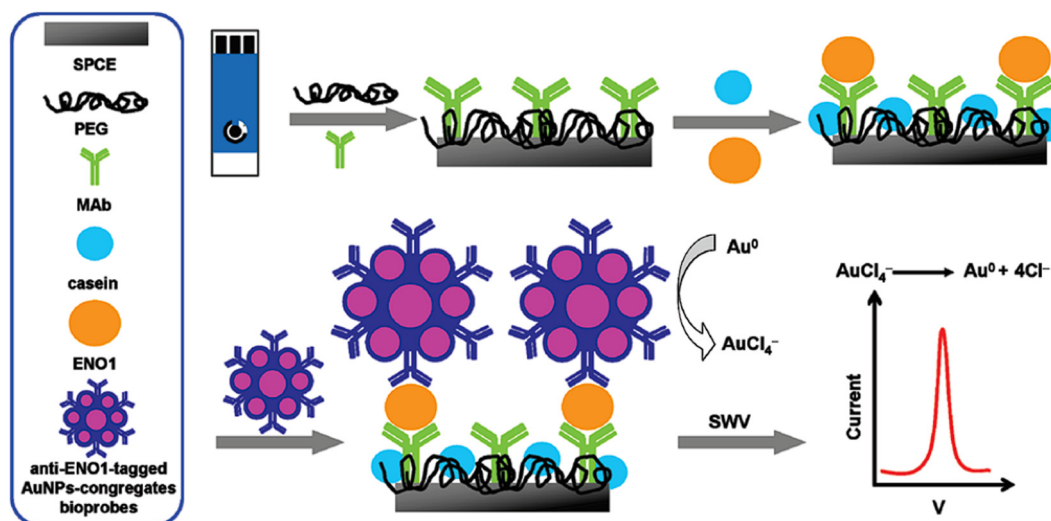


**Figure 4:** Schematic representation of the operation of the electrochemical immunosensor for the detection of ENO1. Reproduced with permission from ref. [47].

antibodies and the carboxylic groups on the material. For example, the carboxylic groups on carbon nanotubes allow covalent bonding to the antibody amine groups through carbodiimide coupling. Similarly, the oxygen-containing functional groups on biochar can react with carbodiimide to form reactive intermediates for covalent attachment of antibodies. Nafion can also be modified on the gold electrode through electrostatic attraction and entrapment of antibodies within its polymer network. The gold electrode surface further enables covalent immobilization of antibodies through self-assembled monolayers. The self-assembled monolayers provide a well-defined interface for carbodiimide coupling of antibodies to the electrode. These various platforms and immobilization strategies on gold screen-printed electrodes – including covalent immobilization, electrostatic interaction and entrapment – offer different advantages in terms of stability, loading capacity, orientation, and ease of implementation for electrochemical immunosensors.

Affinity-based attachment makes use of high affinity non-covalent interaction between specific binding pairs such as biotin/streptavidin, protein A/antibody, and nickel/histidine tag. The binding pair is introduced onto the nanomaterial electrode surface and the capture element is modified with the complementary component [57–59]. For example, a streptavidin-biotin horseradish peroxidase (HRP) complex (SABC) plays an important role in amplifying the signal in the detection of the EGFR mutation status in lung cancer patients [60]. The SABC complexes are prepared by mixing streptavidin-HRP and biotin-HRP together. Streptavidin has four binding sites for biotin. When mixed, the streptavidin binds to biotin-HRP, forming complexes with multiple HRP enzymes. The SABC complexes are then added to the electrode. The biotin binding sites on streptavidin will bind to the biotin on the reporter probes attached to the electrode. This results in many HRP enzymes being brought to the electrode surface through the streptavidin-biotin binding. In the detection step, the HRP catalyzes the oxidation of 3,3',5,5'-tetramethylbenzidine to generate a current signal. Since there are many HRP enzymes accumulated on the electrode due to the SABC method, this greatly amplifies the current signal compared to just having HRP directly conjugated to the probe.

Electrostatic interaction relies on charge-based attraction between positively charged electrode materials like chitosan and polyethyleneimine and negatively charged capture biomolecules [53,61,62]. It is simple, mild, and preserves bioactivity. For example, Lütfi Yola et al. [63] reported a sensor platform was composed of a silicon nitride ( $\text{Si}_3\text{N}_4$ )/ $\text{MoS}_2$  composite coated onto MWCNTs. The  $\text{Si}_3\text{N}_4/\text{MoS}_2$  composite contains polar functional groups that can interact electrostatically with the capture antibody (anti-CYFRA21-1-

Ab1). The capture antibody is immobilized onto the  $\text{Si}_3\text{N}_4/\text{MoS}_2$ -MWCNT modified electrode via electrostatic/ionic interactions between the  $-\text{NH}_2$  groups of the antibody and the polar groups on the  $\text{Si}_3\text{N}_4/\text{MoS}_2$  surface. This electrostatic immobilization provides stable attachment of the capture antibody onto the sensor platform, orienting the antibodies in an optimal position to bind the target antigen. The electrostatic immobilization also helps maintain the bioactivity of the antibody and prevents denaturation. But the electrostatic interaction is relatively weaker making the immobilized antibodies prone to detachment. Changing pH or ionic strength can disrupt the interaction.

In general, covalent attachment and affinity-based strategies result in more stable and reproducible electrochemical immunosensor platforms compared to physical adsorption which is prone to electrode fouling, denaturation, and leakage of capture elements. However, covalent methods can damage biomolecule structure while affinity techniques require additional modification steps.

Ideally, the immobilization approach should provide strong stable attachment, high loading density, uniform oriented capture probe alignment, minimal non-specific adsorption, and retention of biological activity. Overall, a balance between high stability and high bioactivity needs to be met through optimal design of electrode interface and immobilization chemistry. Leveraging the advantages of different strategies is an emerging trend to develop smart “bio-friendly” interfaces for enhanced immunosensor performance.

## 4 Signal amplification approaches

The intrinsic electrochemical signal generated from the biomarker binding event on the immunosensor interface is often not sufficient for sensitive detection, especially at low biomarker concentrations. Hence, signal enhancement strategies are crucial to improve sensor performance in terms of detection limits and linear dynamic range. The aim is to amplify the output electrochemical response per binding event. Common approaches utilize enzymes, nanomaterials, polymers, dendrimers, and DNA nanostructures.

### 4.1 Enzyme labels

Enzyme labels like HRP and glucose oxidase (GOx) are widely coupled to secondary antibodies. The enzyme catalyzes the breakdown of substrates like hydrogen peroxide, producing an electroactive product that amplifies the current or potential response.

For instance, HRP can act as an electron transfer agent to amplify the electrochemical signal [64]. The HRP is conjugated to streptavidin-coated magnetic beads, which allows high loading of HRP on the sensor surface. HRP catalyzes the oxidation of hydroquinone (HQ) by hydrogen peroxide. This reaction generates an electrochemical signal (reduction peak of HQ) that can be measured by voltammetric techniques like square wave voltammetry. The level of HRP on the sensor surface, and consequently the electrochemical signal, depends on the cleavage of the Asp-Glu-Val-Asp (DEVD) peptide by caspase 3. When caspase 3 is present, it cleaves the DEVD peptide, releasing HRP from the surface and decreasing the electrochemical signal. So, by measuring the reduction peak current of HQ, the authors are able to detect caspase 3 activity down to 100 pM. The decrease in peak current correlates to the amount of caspase 3 present.

GOx was used to label the biomarker proteins Annexin II and MUC5AC [65]. The proteins are conjugated to GOx using glutaraldehyde chemistry. When the GOx-labeled proteins bind to their specific antibodies on the sensor surface, the GOx can catalyze glucose oxidation, generating H<sub>2</sub>O<sub>2</sub>. The H<sub>2</sub>O<sub>2</sub> generated is then reduced by the hydrazine catalyst on the sensor surface, producing a measurable current response. So, the GOx provides an electrochemical signal to detect binding of the biomarker proteins. More GOx-labeled protein bound to the sensor surface leads to more H<sub>2</sub>O<sub>2</sub> generation and higher current. Less GOx binding causes lower current. This forms the basis of a competitive assay – unlabeled biomarker proteins compete with GOx-labeled proteins for antibody binding sites. More unlabeled protein leads to less GOx binding and lower current. So, the concentration of unlabeled biomarker protein can be quantified by measuring the reduction in current compared to a baseline with just GOx-labeled protein. GOx amplification of the binding event into a detectable electrochemical signal allows sensitive detection of the biomarker proteins down to pg·mL<sup>-1</sup> levels. In another work [66], GOx catalyzes the oxidation of glucose to generate hydrogen peroxide H<sub>2</sub>O<sub>2</sub>. H<sub>2</sub>O<sub>2</sub> acts as a coreactant to enhance the ECL reaction of luminol. So, the presence of GOx leads to *in situ* production of H<sub>2</sub>O<sub>2</sub> which amplifies the ECL signal. GOx is conjugated to the Ab2. So, when the immunoreaction occurs between the antigen and Ab1, the GOx labeled Ab2 binds as well, bringing GOx to the electrode surface. This increases the amount of GOx near the electrode, generating more H<sub>2</sub>O<sub>2</sub> and enhancing the ECL signal further. GOx is loaded onto graphene along with the ZnO NPs and Ab2. Graphene provides a larger surface area to load more GOx and Ab2, further amplifying the ECL signal.

## 4.2 NP labels

Nanomaterials like AuNPs, CNT, graphene, Co<sub>3</sub>O<sub>4</sub>, etc., can be functionalized with detector antibodies to serve as labels for signal enhancement. Owing to their high conductivity, catalytic properties, and large surface area, they act as nanocarriers to load a high number of detector antibodies and effectively amplify immunosensor response.

For example, Co<sub>3</sub>O<sub>4</sub>@CeO<sub>2</sub>-Au@Pt nanocomposite has been used as enzyme-mimetic labels [67]. Co<sub>3</sub>O<sub>4</sub> nanocubes have excellent electrocatalytic activity towards the reduction of H<sub>2</sub>O<sub>2</sub>. CeO<sub>2</sub> NPs further enhance the catalytic performance of Co<sub>3</sub>O<sub>4</sub> due to a synergistic effect. Au@Pt NPs also have good electrocatalytic properties for H<sub>2</sub>O<sub>2</sub> reduction. Combining Au@Pt with Co<sub>3</sub>O<sub>4</sub>@CeO<sub>2</sub> results in a nanocomposite with superior catalytic activity compared to the individual components. The Co<sub>3</sub>O<sub>4</sub>@CeO<sub>2</sub> core-shell structure provides a large surface area for loading the Au@Pt NPs. This increases the amount of nanocomposite that can bind to the secondary antibody and thus enhances the catalytic current signal. The nanocomposite improves electron transfer efficiency on the electrode surface, leading to higher sensitivity. Co<sub>3</sub>O<sub>4</sub>@CeO<sub>2</sub>-Au@Pt exhibits enzyme-mimetic catalytic activity similar to HRP towards H<sub>2</sub>O<sub>2</sub> reduction. Using the nanocomposite instead of HRP helps avoid instability issues associated with enzyme labels. The synergistic effect and enhanced catalytic properties of the Co<sub>3</sub>O<sub>4</sub>@CeO<sub>2</sub>-Au@Pt nanocomposite allow it to act as an enzyme-mimetic label to amplify the electrochemical signal and improve detection sensitivity for the immunosensor.

## 4.3 Dendrimers

Dendrimers are highly branched globular macromolecules with numerous surface groups that can conjugate to signal molecules like enzymes, metals, NPs, and redox markers. The three-dimensional architecture provides a high loading capacity. For example, Idris et al. [68] reported that immunosensor is based on an exfoliated graphite electrode modified with a nanocomposite of carbon nanodots (CNDTs) and polypropylene imine dendrimer (PPI) (Figure 5). The dendrimer plays an important role in the sensor. The PPI dendrimer was electrodeposited onto the electrode surface modified with CNDTs. It increases the surface area of the electrode for higher antibody loading. Its spherical morphology and surface functional groups facilitate immobilization of the antibody through both electrostatic and host-guest interactions. It improves conductivity and accelerates electron transfer kinetics at the electrode interface. Its

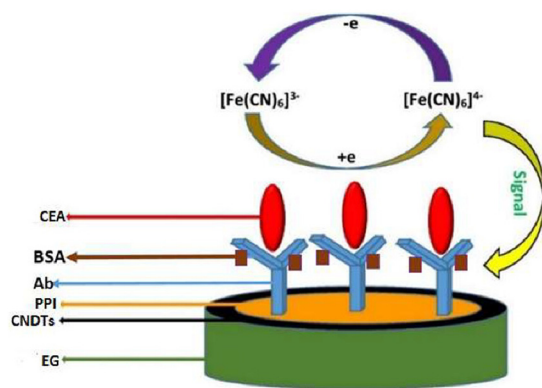


**Figure 5:** Processes involved in the preparation of the immunosensor. Reproduced with permission from ref. [68].

biocompatibility helps maintain the bioactivity of the antibody for improved analyte binding. Together with the CNDTs, the dendrimer-CNDT nanocomposite synergistically enhances the electrochemical signal. This results in higher sensitivity with a low detection limit of  $0.00145 \text{ ng}\cdot\text{mL}^{-1}$  for CEA.

#### 4.4 DNA nanostructures

Self-assembled DNA nanoarchitectures such as tetrahedrons, nanoflowers, nanoribbons, and nanocages can integrate numerous enhancer moieties like redox reporters, enzymes, and NPs onto their large surface area. Hybridization chain reaction or strand displacement amplification using functional DNA structures can also produce a cascading signal enhancement effect. For example, Liu et al. [69] described the development of an electrochemical biosensor for detecting lung cancer-related microRNAs using 3D DNA origami nanostructures. The sensor uses a 3D DNA tetrahedron structure as the base. This tetrahedron has three thiol groups that allow it to self-assemble on a gold electrode surface. A DNA strand with a stem-loop structure is attached to the top of the tetrahedron. The loop portion is complementary to the target microRNA. The stem part contains a ferrocene tag for electrochemical signaling. When the target microRNA hybridizes to the loop, it opens up the stem-loop structure. This moves the ferrocene tag closer to the electrode surface, increasing the electrochemical signal. The 3D tetrahedron structure provides a scaffold to correctly orient the signaling stem-loop probe on the surface. It also provides some distance between the ferrocene tag and the electrode, making the “signal-on” sensing mechanism possible. Without the 3D nanostructure, the stem-loop probe would lie flat on the surface. The ferrocene would already be close to the electrode, so target hybridization would not change the signal as much. This amplifies the current or potential response by

several orders of magnitude. However, DNA nanoassembly requires optimization and the structures may degrade under harsh experimental conditions.

## 5 Applications for major lung cancer biomarkers

Owing to their high sensitivity, selectivity, and affordability, electrochemical immunosensors have been widely applied for detecting common protein and genetic lung cancer biomarkers. The use of advanced nanomaterials and signal enhancement strategies has enabled improvements in key analytical performance parameters such as detection limits, linear ranges, and anti-interference capabilities.

### 5.1 CEA

CEA is an important broad-spectrum tumor marker upregulated in lung cancer. Electrochemical immunosensors have been developed targeting CEA for early diagnosis. For instance, Wang et al. [70] reported an electrochemical immunosensor for detecting the CEA. The immunosensor is constructed on a fluorine-doped tin oxide electrode modified with a composite of PANI-loaded few-layered MXene (MXene@PANI). AuNPs and  $\beta$ -cyclodextrin (Au- $\beta$ -CD) are further electrodeposited on the surface to immobilize anti-CEA antibodies (Figure 6a). This sensor exhibits excellent performance for CEA detection with a wide linear detection range of  $0.5\text{--}350 \text{ ng}\cdot\text{mL}^{-1}$  and a low limit of detection of  $0.0429 \text{ ng}\cdot\text{mL}^{-1}$ . The high conductivity of the MXene@PANI composite and the capability of Au- $\beta$ -CD to efficiently immobilize antibodies contribute to the sensor's sensitivity. The immunosensor also demonstrates good selectivity, reproducibility, and stability. Furthermore, it shows feasibility for detecting CEA in human serum samples, with recovery ratios of 97.52–103.98%. Gan et al. [71] described a similar electrochemical immunosensor for detecting CEA. The immunosensor uses magnetic DNA-tagged nanoprobes made of zirconia/iron oxide NPs bound to DNA and antibodies. When the sensor detects CEA, it forms a sandwich structure with capture antibodies on the sensor surface, CEA, and the antibody-bound nanoprobes (Figure 6b). The large amount of enzyme horseradish peroxidase on the nanoprobes amplifies the signal. This sensor was able to detect CEA at concentrations as low as  $5 \text{ pg}\cdot\text{mL}^{-1}$ , which is 100 times more sensitive than conventional ELISA methods. Testing on human serum samples showed good accuracy compared to ELISA.

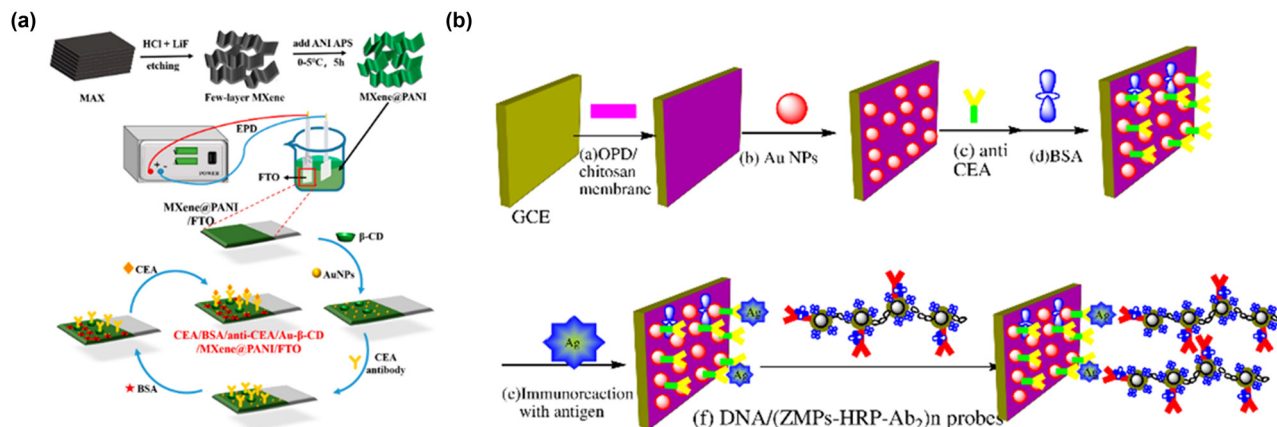


**Figure 6:** Several electrochemical sensors for CEA detection. (a) PANI-loaded MXene and gold-decorated  $\beta$ -cyclodextrin. (b) DNA/(ZMPs-HRP-CEA Ab2)n. Reproduced with permission from ref. [70,71].

## 5.2 NSE

NSE is an important biomarker upregulated in lung cancer tissues. Wang et al. [72] developed a sensitive electrochemical immunosensor using a  $\text{MoS}_2$ @Au nanzyme label for detecting the biomarker NSE. The  $\text{MoS}_2$  nanoflowers provided abundant sites to load Au nanoclusters which catalyzed  $\text{H}_2\text{O}_2$  decomposition to amplify the amperometric signal. The NSE antibody was coupled to the  $\text{MoS}_2$ @Au nanzyme while the capture antibody was immobilized on reduced graphene oxide (Figure 7). The immunosensor detected NSE from  $0.1 \text{ pg}\cdot\text{mL}^{-1}$  to  $10 \text{ ng}\cdot\text{mL}^{-1}$  with a low

detection limit of  $0.05 \text{ pg}\cdot\text{mL}^{-1}$ . It showed good selectivity against other proteins, reproducibility of 1.51% RSD, and stability for 48 hours. The sensor was successfully applied to NSE detection in spiked serum samples with recoveries from 97.6% to 99.9%. The  $\text{MoS}_2$ @Au nanzyme label enhanced sensitivity and the performance indicates that this electrochemical immunosensor has potential for clinical diagnosis of NSE.

Karaman et al. [73] described the development of a highly sensitive electrochemical immunosensor for detecting NSE. The immunosensor uses a GCE modified with AuNPs-decorated graphene and  $\text{MoS}_2$  nanocomposites as the sensor

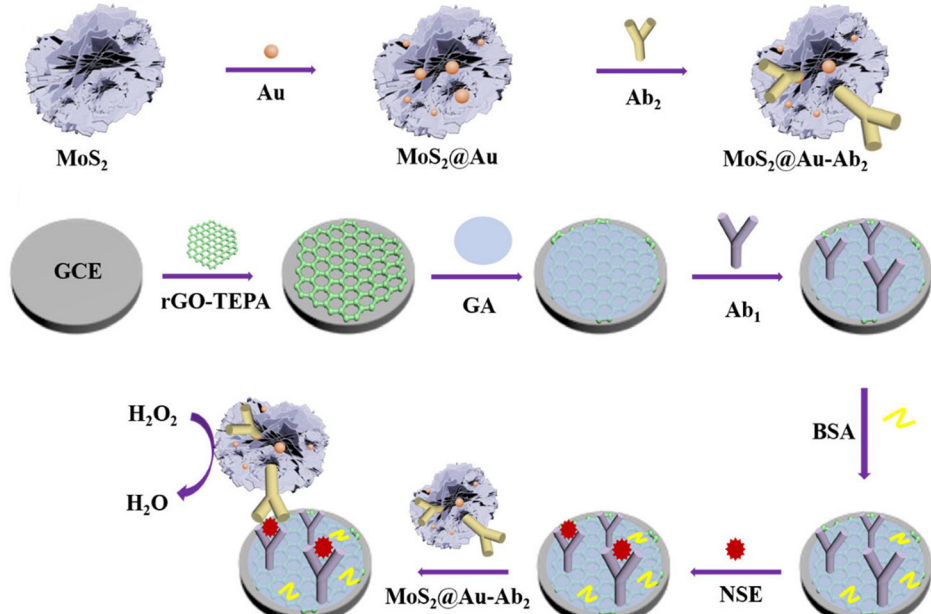


**Figure 7:**  $\text{MoS}_2$ @Au-Ab2 bioconjugate for NSE detection. Reproduced with permission from ref. [72].

platform. This provides a large surface area for antibody binding. The signal is amplified using a cobalt iron oxide-silver nanocomposite, which binds to secondary antibodies. The immunosensor showed excellent performance for NSE detection with a wide linear range from 0.01 to 1  $\text{pg}\cdot\text{mL}^{-1}$  and a low limit of detection of 3  $\text{fg}\cdot\text{mL}^{-1}$ . It also demonstrated high selectivity against interfering proteins and stability over a 7-week period. Han et al. [74] used a signal amplification strategy based on the electrocatalytic properties of nickel hexacyanoferrate nanoparticles (NiHCFNPs) towards dopamine oxidation. The sensor is fabricated by modifying a glassy carbon electrode with a film of porous gold nanocrystals, followed by NiHCFNPs and then a layer of AuNPs-functionalized graphene nanosheets (Au-Gra). This provides a large surface area for antibody loading. In the presence of dopamine, the NiHCFNPs greatly enhance the oxidation current response. This amplification allows sensitive detection of NSE down to 0.3  $\text{pg}\cdot\text{mL}^{-1}$ , with a wide linear range from 0.001–100  $\text{ng}\cdot\text{mL}^{-1}$ . The immunosensor exhibits high selectivity, reproducibility, and stability. Testing on clinical samples shows good agreement with standard ELISA results.

### 5.3 CYFRA 21-1

CYFRA 21-1 is an important NSCLC biomarker. A novel immunosensor was reported based on a hydroxyapatite-

chitosan nanocomposite platform and dendritic CuS NPs label. Kumar et al. [75] reported on the development of a highly sensitive electrochemical biosensor for the detection of the oral cancer biomarker CYFRA-21-1. The biosensor uses a nanostructured yttrium oxide ( $\text{nY}_2\text{O}_3$ ) platform functionalized with antibodies specific for CYFRA-21-1. Structural characterization shows successful synthesis of oval-shaped  $\text{nY}_2\text{O}_3$  NPs around 80 nm in size. The  $\text{nY}_2\text{O}_3$  was electrophoretically deposited onto an ITO electrode and the antibodies were immobilized using EDC-NHS chemistry (Figure 8). Testing shows that the biosensor exhibits a wide linear detection range from 0.01 to 50  $\text{ng}\cdot\text{mL}^{-1}$  CYFRA-21-1, with a remarkably low limit of detection of 0.01  $\text{ng}\cdot\text{mL}^{-1}$ . The biosensor demonstrates high sensitivity of  $226.0 \Omega\cdot\text{mL}\cdot\text{ng}^{-1}$ . Analysis of saliva samples shows good correlation between the biosensor and ELISA for detecting CYFRA-21-1 levels.

Aydin et al. [76] presented a new electrochemical biosensor for detecting the lung cancer biomarker CYFRA 21-1. The biosensor uses an ITO electrode modified with a multi-layer film consisting of electrodeposited AuNPs and an electropolymerized amino-substituted pyrrole polymer (P (PyAmn)). The AuNPs provide high conductivity and the P (PyAmn) polymer provides a large surface area for antibody immobilization. The biosensor detects CYFRA 21-1 through specific binding to anti-CYFRA 21-1 antibodies on the surface, which causes an increase in impedance measured by EIS. The biosensor demonstrated a wide linear detection range from 0.015–90  $\text{pg}\cdot\text{mL}^{-1}$ , a low detection

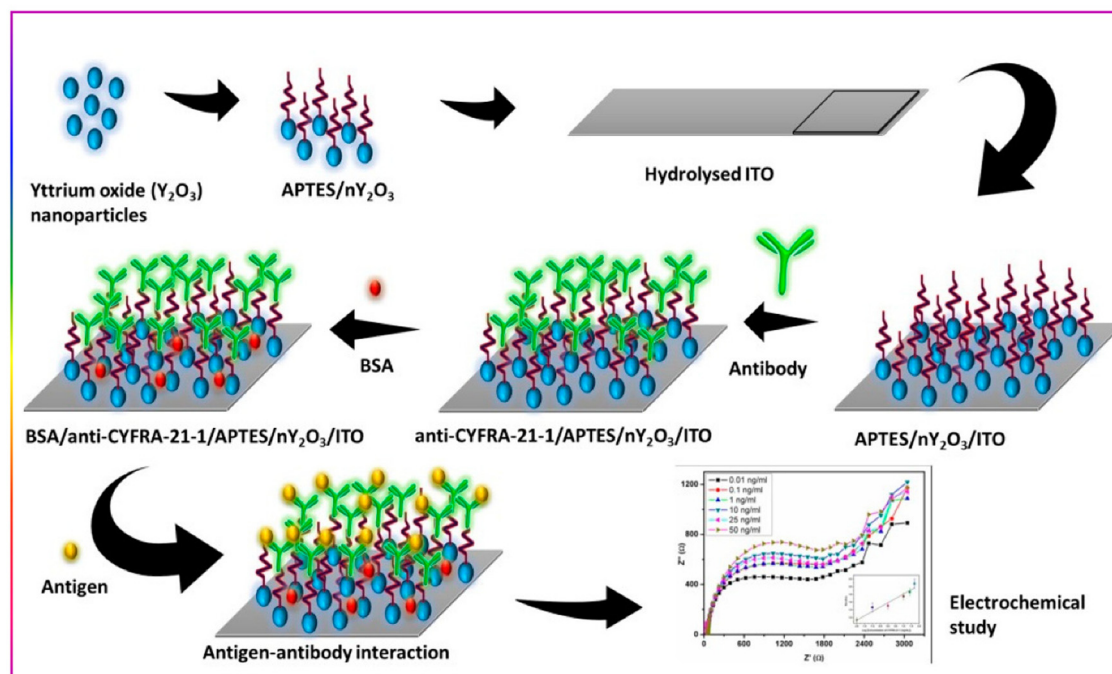


Figure 8: Stepwise fabrication process of the BSA/anti-CYFRA-21-1/APTES/nY<sub>2</sub>O<sub>3</sub>/ITO biosensor. Reproduced with permission from ref. [75].

limit of  $4.59 \text{ fg}\cdot\text{mL}^{-1}$ . It showed high selectivity for CYFRA 21-1 over other proteins. The biosensor was successfully applied to detect spiked CYFRA 21-1 in human serum samples with recoveries of 95.47–106.70%. Lu et al. [77] utilized a ring-opening polymerization (ROP) amplification strategy to greatly improve detection sensitivity. The immunosensor is fabricated by immobilizing capture antibodies onto a gold electrode modified with a self-assembled monolayer. After CYFRA 21-1 binds to the capture antibodies, detection antibodies are added, which initiates the ROP reaction. This results in a large number of electroactive ferrocene molecules becoming attached to the detection antibodies, amplifying the detection signal. Using this ROP amplification strategy, the immunosensor demonstrated a low detection limit of  $9.08 \text{ fg}\cdot\text{mL}^{-1}$  for CYFRA 21-1, which is 100–1,000 times lower than other reported methods. The immunosensor also showed excellent selectivity against other proteins, a wide linear detection range of  $1 \text{ pg}\cdot\text{mL}^{-1}$  to  $1 \mu\text{g}\cdot\text{mL}^{-1}$ , and good accuracy for the detection of clinical serum samples.

## 5.4 Emerging biomarkers

In addition to conventional markers, immunosensors have also targeted emerging lung cancer biomarkers. For instance, progastrin-releasing peptide (ProGRP) is an important biomarker for lung cancer diagnosis and monitoring, especially in early stages [78]. The immunosensor utilizes antibodies specific to ProGRP immobilized on the electrode surface. The interaction between ProGRP and the antibodies causes measurable changes in electrical signals that correlate with ProGRP concentration. The modified electrode provides a large surface area and optimal environment for antibody binding. The immunosensor demonstrated high sensitivity with a detection limit of  $0.133 \text{ ng}\cdot\text{mL}^{-1}$  ProGRP, along with excellent reproducibility and storage stability over 30 days.

VEGF165 plays a key role in tumor angiogenesis and metastasis in lung cancer. Amouzadeh Tabrizi et al. [79] described the development of a novel electrochemical aptasensor for the sensitive and selective detection of VEGF165. The aptasensor is based on an anti-VEGF165 aptamer immobilized on a screen-printed electrode modified with ordered mesoporous carbon-gold nanocomposite. The aptasensor detected VEGF165 through changes in interfacial electron transfer resistance measured by electrochemical impedance spectroscopy. The sensor exhibited a wide linear detection range from  $10.0$  to  $300 \text{ pg}\cdot\text{mL}^{-1}$  and a low limit of detection of  $1 \text{ pg}\cdot\text{mL}^{-1}$ .

Detecting microRNAs (miRNAs) like miR-21 holds immense importance in lung cancer diagnostics due to their stability and

regulatory roles. Liu et al. [80] reported a novel electrochemical biosensing platform based on a hybrid DNA hydrogel, which was developed for the sensitive detection of lung cancer-specific miR-21. The biosensor utilized ferrocene-tagged DNA recognition probes that, when hybridized with miR-21, led to the dissolution of the DNA hydrogel, causing a reduction in current detectable by cyclic and differential pulse voltammetry. Notably, the biosensor exhibited a remarkable detection limit of  $5 \text{ nM}$  for miR-21, along with a linear range of detection spanning from  $10 \text{ nM}$  to  $50 \mu\text{M}$ . Importantly, the biosensor showcased high specificity for miR-21 over interfering sequences, demonstrating its potential for selective clinical diagnosis.

The study by Xu et al. [81] revolved around the significance of detecting the EGFR exon 19 status in lung cancer, as patients with exon 19 deletions often exhibit greater sensitivity to EGFR tyrosine kinase inhibitors than those with other EGFR mutations. By analyzing the conversations, it is evident that the utilization of deep learning techniques, particularly the Bidirectional Long Short-Term Memory model, proves to be effective in automating the detection of EGFR exon 19 deletions. This model, trained on a substantial dataset of patient genomic sequences, demonstrates excellent performance in terms of accuracy, sensitivity, and specificity, outperforming previous methods such as Amplification Refractory Mutation System PCR.

## 6 Trends and future outlook

While electrochemical immunosensors have shown immense potential for sensitive detection of lung cancer biomarkers, there are ongoing efforts to further enhance their viability and bring the technology closer to widespread clinical adoption.

Simultaneous detection of multiple biomarkers on a single integrated platform can provide more reliable diagnosis compared to measuring any single biomarker. Multiplexing offers a promising approach to account for the complexity and heterogeneity of lung cancers. For instance, nanocomposite interfaces capable of spatially isolating different antibodies or aptamers allow simultaneous measurement of markers like CEA, NSE, CYFRA21-1 on the same electrode. The use of unique electroactive labels for each biomarker enables discrimination by voltammetric peak potential. Arrays of individually addressable electrodes facilitate parallel multiplexed sensing. Multiplexing technology needs further innovation to increase panel size and assay speed. But the capability to profile expression patterns of different lung cancer biomarkers would aid in early diagnosis and personalized therapy.

Point-of-care devices are increased impetus on developing miniaturized point-of-care diagnostic devices for rapid, on-site detection of lung cancer biomarkers. Embedding electrochemical immunosensors with microfluidics and electronics into portable, inexpensive handheld gadgets and microchips would enable decentralized testing. Integrated microfluidic systems allow automated sample handling. Handheld potentiostats linked to smartphones or tablets provide data acquisition and connectivity. 3D printing can produce low-cost immunoassay devices for resource-limited settings. However, seamless integration and operational robustness remain challenges.

Wearable electrochemical biosensors can allow continuous non-invasive monitoring of clinically relevant biomarkers. Flexible and stretchable platforms based on fabrics, tattoos, and patches with embedded immunosensors are being designed. For instance, screen-printed electrodes on stretchable substrates have been applied. Wireless sensors for real-time tracking of lung cancer markers in sweat or saliva could provide valuable diagnostic information and aid in longitudinal disease management. However, reproducibly manufacturing flexible sensor strips and minimizing noise from motion artifacts require further research.

Microfluidic microchips offer automation, miniaturization, and multiplexing capabilities. Immunosensors coupled to microfluidic platforms enhance kinetic analysis, allow *in situ* calibration, and reduce sample volumes and reagent consumption. Sensing and sample preparation can be integrated onto compact Lab-on-a-Chip type devices for point-of-care use.

Very few electrochemical immunosensors for cancer biomarkers have been commercially translated so far. This is due to practical challenges such as reproducibility across fabrication batches, device stability under variable conditions, selectivity in complex samples like whole blood, and stringent clinical validation. Academic and industry partnerships focused on overcoming these limitations to develop market-ready products need to be fostered by leveraging the expertise of different stakeholders. Increased commercialization and regulatory approval would drive wider clinical acceptance and make the devices viable diagnostic tools for lung cancer.

In addition, there are several factors to consider when choosing the appropriate electroanalytical technique for specific biomarkers or clinical scenarios. The type of biomarker, required sensitivity, sample matrix, and purpose of testing need to be balanced to identify the most appropriate technique. Impedance spectroscopy has been widely used for detecting DNA and RNA biomarkers due to its high sensitivity to surface binding events, while amperometry

and voltammetry are commonly employed for protein biomarkers due to their compatibility with enzyme labels and NPs tags. Techniques like impedance spectroscopy and voltammetry tend to achieve lower detection limits, making them well suited for detecting biomarkers at low concentrations. However, amperometry can also achieve high sensitivity when combined with amplification strategies. Some techniques may be more tolerant of complex matrices like blood and serum samples. For instance, impedance spectroscopy has demonstrated good anti-interference capabilities in complex media. Certain scenarios may prioritize parameters like speed, cost, or portability. For example, amperometry is often favored for point-of-care applications due to its simplicity and compatibility with miniaturized devices. Meanwhile, impedance spectroscopy can offer label-free, real-time monitoring capabilities suitable for longitudinal studies.

## 7 Conclusion

Electrochemical immunosensors show promise for sensitive lung cancer diagnosis. Nanomaterials like graphene and metal NPs enhance sensor performance by increasing surface area and conductivity. Advanced antibody immobilization and signal amplification strategies improve sensitivity. Recent sensors have achieved detection limits in the femtogram per milliliter range for biomarkers like CEA and miRNAs. However, multiplexed detection of multiple biomarkers, point-of-care devices, and wearable platforms could further improve clinical viability. While current research has made impressive progress, commercialization, standardization and clinical validation are essential next steps to translate these sensors into products for regulatory approval and real-world use. Widespread adoption depends on addressing remaining challenges through multidisciplinary efforts.

In summary, electrochemical immunosensors represent a powerful platform for early lung cancer detection and monitoring. Their ability to detect biomarkers at extremely low levels holds promise for improving patient outcomes through earlier diagnosis and treatment. However, further research and development is needed to realize this potential, from enhancing sensor performance to facilitating clinical integration. With a concerted push from both academia and industry, electrochemical immunosensors could transform lung cancer management in the coming years.

**Funding information:** Authors state no funding involved.

**Author contributions:** Li Fu: writing – original draft, writing – review and editing, methodology, and formal analysis; Xiaozhu Liu: writing – review and editing, formal analysis, and project administration; Junyi Cao: writing – original draft, writing – review and editing, and methodology; Huan Li: writing – original draft; Anyou Xie: formal Analysis; and Yue Liu: writing – review and editing and project administration.

**Conflict of interest:** Authors state no conflict of interest.

**Data availability statement:** Data sharing is not applicable to this article as no datasets were generated or analyzed during the current study.

## References

[1] Howlader N, Forjaz G, Mooradian MJ, Meza R, Kong CY, Cronin KA, et al. The effect of advances in lung-cancer treatment on population mortality. *N Engl J Med.* 2020;383(7):640–9. doi: 10.1056/NEJMoa1916623.

[2] Bade BC, Cruz CSD. Lung cancer 2020: Epidemiology, etiology, and prevention. *Chest Med.* 2020;41(1):1–24. doi: 10.1016/j.ccm.2019.10.001.

[3] Schabath MB, Cote ML. Cancer progress and priorities: lung cancer. *Cancer Epidemiol Biomarkers Prev.* 2019;28(10):1563–79. doi: 10.1158/1055-9965.EPI-19-0221.

[4] Noorelddeen R, Bach H. Current and future development in lung cancer diagnosis. *Int J Mol Sci.* 2021;22(16):8661. doi: 10.3390/ijms22168661.

[5] Yang D, Liu Y, Bai C, Wang X, Powell CA. Epidemiology of lung cancer and lung cancer screening programs in China and the United States. *Cancer Lett.* 2020;468:82–7. doi: 10.1016/j.canlet.2019.10.009.

[6] Wang M, Herbst RS, Boshoff C. Toward personalized treatment approaches for non-small-cell lung cancer. *Nat Med.* 2021;27(8):1345–56. doi: 10.1038/s41591-021-01450-2.

[7] Sharma P, Mehta M, Dhanjal DS, Kaur S, Gupta G, Singh H, et al. Emerging trends in the novel drug delivery approaches for the treatment of lung cancer. *Chem-Biol Interact.* 2019;309:108720. doi: 10.1016/j.cbi.2019.06.033.

[8] Biswas M, Ades A, Hamilton W. Symptom lead times in lung and colorectal cancers: what are the benefits of symptom-based approaches to early diagnosis? *Br J Cancer.* 2015;112(2):271–7.

[9] Herath S, Sadeghi Rad H, Radfar P, Ladwa R, Warkiani M, O’Byrne K, et al. The role of circulating biomarkers in lung cancer. *Front Oncol.* 2022;11:801269.

[10] Sanjayan CG, Ravikumar CH, Balakrishna RG. Perovskite QD based paper microfluidic device for simultaneous detection of lung cancer biomarkers – Carcinoembryonic antigen and neuron specific enolase. *Chem Eng J.* 2023;464:142581. doi: 10.1016/j.cej.2023.142581.

[11] Tian Z, Liang C, Zhang Z, Wen H, Feng H, Ma Q, et al. Prognostic value of neuron-specific enolase for small cell lung cancer: a systematic review and meta-analysis. *World J Surgical Oncol.* 2020;18(1):116. doi: 10.1186/s12957-020-01894-9.

[12] Fu L, Wang R, Yin L, Shang X, Zhang R, Zhang P. CYFRA21-1 tests in the diagnosis of non-small cell lung cancer: A meta-analysis. *Int J Biol Markers.* 2019;34(3):251–61. doi: 10.1177/1724600819868234.

[13] Wang W, Li X, Liu C, Zhang X, Wu Y, Diao M, et al. MicroRNA-21 as a diagnostic and prognostic biomarker of lung cancer: a systematic review and meta-analysis. *Biosci Rep.* 2022;42(5):BSR20211653. doi: 10.1042/BSR20211653.

[14] Esposito Abate R, Frezzetti D, Maiello MR, Gallo M, Camerlingo R, De Luca A, et al. Next generation sequencing-based profiling of cell free DNA in patients with advanced non-small cell lung cancer: Advantages and pitfalls. *Cancers.* 2020;12(12):3804. doi: 10.3390/cancers12123804.

[15] Koh Y, Yagi S, Akamatsu H, Kanai K, Hayata A, Tokudome N, et al. Heterogeneous expression of programmed death receptor-ligand 1 on circulating tumor cells in patients with lung cancer. *Clin Lung Cancer.* 2019;20(4):270–7.e1. doi: 10.1016/j.clc.2019.03.004.

[16] Khalid MAU, Kim YS, Ali M, Lee BG, Cho Y-J, Choi KH. A lung cancer-on-chip platform with integrated biosensors for physiological monitoring and toxicity assessment. *Biochem Eng J.* 2020;155:107469. doi: 10.1016/j.bej.2019.107469.

[17] Usman F, Dennis JO, Aljameel AI, Ali MKM, Aldaghri O, Ibnaouf KH, et al. Plasmonic biosensors for the detection of lung cancer biomarkers: A review. *Chemosensors.* 2021;9(11):326. doi: 10.3390/chemosensors9110326.

[18] Khanmohammadi A, Aghaie A, Vahedi E, Qazvini A, Ghanei M, Afkhami A, et al. Electrochemical biosensors for the detection of lung cancer biomarkers: A review. *Talanta.* 2020;206:120251. doi: 10.1016/j.talanta.2019.120251.

[19] Deepa Nohwal B, Pundir C. An electrochemical CD59 targeted noninvasive immunosensor based on graphene oxide nanoparticles embodied pencil graphite for detection of lung cancer. *Microchem J.* 2020;156:104957. doi: 10.1016/j.microc.2020.104957.

[20] Tao D, Gu Y, Song S, Nguyen EP, Cheng J, Yuan Q, et al. Ultrasensitive detection of alpha-synuclein oligomer using a PolyD-glucosamine/gold nanoparticle/carbon-based nanomaterials modified electrochemical immunosensor in human plasma. *Microchem J.* 2020;158:105195. doi: 10.1016/j.microc.2020.105195.

[21] Xiao H, Wei S, Chen Z, Cao L. Label-free electrochemical immuno-sensor based on gold and iron-oxide nanoparticle co-modified rGO-TEPA hybrid for sensitive detection of carcinoembryonic antigen. *Electrocatalysis.* 2020;11(5):513–21. doi: 10.1007/s12678-020-00604-z.

[22] Brazaca LC, dos Santos PL, de Oliveira PR, Rocha DP, Stefano JS, Kalinke C, et al. Biosensing strategies for the electrochemical detection of viruses and viral diseases – A review. *Anal Chim Acta.* 2021;1159:338384. doi: 10.1016/j.aca.2021.338384.

[23] Popov A, Brasius B, Kausaite-Minkstiene A, Ramanaviciene A. Metal nanoparticle and quantum dot tags for signal amplification in electrochemical immunosensors for biomarker detection. *Chemosensors.* 2021;9(4):85. doi: 10.3390/chemosensors9040085.

[24] Kaya SI, Ozcelikay G, Mollarasouli F, Bakirhan NK, Ozkan SA. Recent achievements and challenges on nanomaterial based electrochemical biosensors for the detection of colon and lung cancer biomarkers. *Sens Actuators B: Chem.* 2022;351:130856. doi: 10.1016/j.snb.2021.130856.

[25] Chen X, Jia X, Han J, Ma J, Ma Z. Electrochemical immunosensor for simultaneous detection of multiplex cancer biomarkers based on

graphene nanocomposites. *Biosens Bioelectron*. 2013;50:356–61. doi: 10.1016/j.bios.2013.06.054.

[26] Xu H, Wang Y, Wang L, Song Y, Luo J, Cai X. A label-free micro-electrode array based on one-step synthesis of chitosan–multi-walled carbon nanotube–thionine for ultrasensitive detection of carcinoembryonic antigen. *Nanomaterials*. 2016;6(7):132. doi: 10.3390/nano6070132.

[27] Gu Y, Gong G, Jiang Y, Qin J, Mei Y, Han J. Electrochemical immunosensor modified with nitrogen-doped reduced graphene oxide@Carboxylated multi-walled carbon Nanotubes/Chitosan@Gold nanoparticles for CA125 detection. *Chemosensors*. 2022;10(7):272. doi: 10.3390/chemosensors10070272.

[28] Sobhan A, Jia F, Kelso LC, Biswas SK, Muthukumarappan K, Cao C, et al. A novel activated biochar-based immunosensor for rapid detection of *E. coli* O157:H7. *Biosensors*. 2022;12(10):908. doi: 10.3390/bios12100908.

[29] Li Y, Xu R, Wang H, Xu W, Tian L, Huang J, et al. Recent advances of biochar-based electrochemical sensors and biosensors. *Biosensors*. 2022;12(6):377. doi: 10.3390/bios12060377.

[30] Cancelliere R, Cianciaruso M, Carbone K, Micheli L. Biochar: A sustainable alternative in the development of electrochemical printed platforms. *Chemosensors*. 2022;10(8):344. doi: 10.3390/chemosensors10080344.

[31] Cancelliere R, Di Tinno A, Di Lellis AM, Contini G, Micheli L, Signori E. Cost-effective and disposable label-free voltammetric immunosensor for sensitive detection of interleukin-6. *Biosens Bioelectron*. 2022;213:114467. doi: 10.1016/j.bios.2022.114467.

[32] Hu K, Cheng J, Wang K, Zhao Y, Liu Y, Yang H, et al. Sensitive electrochemical immunosensor for CYFRA21-1 detection based on AuNPs@MoS<sub>2</sub>@Ti<sub>3</sub>C<sub>2</sub>Tx composites. *Talanta*. 2022;238:122987. doi: 10.1016/j.talanta.2021.122987.

[33] Nguyen N-V, Jen C-P. Selective detection of human lung adenocarcinoma cells based on the aptamer-conjugated self-assembled monolayer of gold nanoparticles. *Micromachines*. 2019;10(3):195. doi: 10.3390/mi10030195.

[34] Cheng H, Lai G, Fu L, Zhang H, Yu A. Enzymatically catalytic deposition of gold nanoparticles by glucose oxidase-functionalized gold nanoprobe for ultrasensitive electrochemical immunoassay. *Biosens Bioelectron*. 2015;71:353–8.

[35] Asadzadeh-Firouzabadi A, Zare HR. Preparation and application of AgNPs/SWCNTs nanohybrid as an electroactive label for sensitive detection of miRNA related to lung cancer. *Sens Actuators B: Chem*. 2018;260:824–31. doi: 10.1016/j.snb.2017.12.195.

[36] Jafari-Kashi A, Rafiee-Pour H-A, Shabani-Nooshabadi M. A new strategy to design label-free electrochemical biosensor for ultrasensitive diagnosis of CYFRA 21-1 as a biomarker for detection of non-small cell lung cancer. *Chemosphere*. 2022;301:134636. doi: 10.1016/j.chemosphere.2022.134636.

[37] Lv X, Bi M, Xu X, Li Y, Geng C, Cui B, et al. An ultrasensitive ratio-metric immunosensor based on the ratios of conjugated distyrylbenzene derivative nanosheets with AIECL properties and electrochemical signal for CYFRA21-1 detection. *Anal Bioanal Chem*. 2022;414(3):1389–402. doi: 10.1007/s00216-021-03764-z.

[38] Wang Y, Zhao G, Zhang Y, Pang X, Cao W, Du B, et al. Sandwich-type electrochemical immunosensor for CEA detection based on Ag/MoS<sub>2</sub>@Fe<sub>3</sub>O<sub>4</sub> and an analogous ELISA method with total internal reflection microscopy. *Sens Actuators B: Chem*. 2018;266:561–9. doi: 10.1016/j.snb.2018.03.178.

[39] Mavrič T, Benciná M, Imani R, Junkar I, Valant M, Kralj-Iglič V, et al. Chapter three - electrochemical biosensor based on TiO<sub>2</sub> nanomaterials for cancer diagnostics. In: Iglič A, Rappolt M, García-Sáez AJ, editors. *Advances in biomembranes and lipid self-assembly*. Academic Press; 2018. p. 63–105.

[40] Che W, Zhao X, Wang F, Ma T, Zhao K. Electrochemical detection of CEA and CA153 lung cancer markers based on ZnO/porous graphene oxide composite biosensor. *Int J Electrochem Sci*. 2022;17(12):221272. doi: 10.20964/2022.12.70.

[41] Yu X, Li X, Zhang S, Jia Y, Xu Z, Li X, et al. Ultrasensitive electrochemical detection of neuron-specific enolase based on spiny core-shell Au/CuxO@CeO<sub>2</sub> nanocubes. *Bioelectrochemistry*. 2021;138:107693. doi: 10.1016/j.bioelechem.2020.107693.

[42] Park Y, Hong M-S, Lee W-H, Kim J-G, Kim K. Highly sensitive electrochemical aptasensor for detecting the VEGF165 tumor marker with PANI/CNT nanocomposites. *Biosensors*. 2021;11(4):114. doi: 10.3390/bios11040114.

[43] Kivrak E, Ince-Yardimci A, İlhan R, Kirmizibayrak PB, Yilmaz S, Kara P. Aptamer-based electrochemical biosensing strategy toward human non-small cell lung cancer using polyacrylonitrile/polypyrrole nanofibers. *Anal Bioanal Chem*. 2020;412(28):7851–60. doi: 10.1007/s00216-020-02916-x.

[44] Yen Y-K, Chao C-H, Yeh Y-S. A graphene-PEDOT:PSS modified paper-based aptasensor for electrochemical impedance spectroscopy detection of tumor marker. *Sensors*. 2020;20(5):1372. doi: 10.3390/s20051372.

[45] Chen F, Fan Z, Zhu Y, Sun H, Yu J, Jiang N, et al. β-cyclodextrin-immobilized Ni/graphene electrode for electrochemical enantiorrecognition of phenylalanine. *Materials*. 2020;13(3):777.

[46] Zhang W, Yang J, Wu D. Surface-functionalized MoS<sub>2</sub> nanosheets sensor for direct electrochemical detection of PIK3CA gene related to lung cancer. *J Electrochem Soc*. 2020;167(2):027501.

[47] Ho JA, Chang H-C, Shih N-Y, Wu L-C, Chang Y-F, Chen C-C, et al. Diagnostic detection of human lung cancer-associated antigen using a gold nanoparticle-based electrochemical immunosensor. *Anal Chem*. 2010;82(14):5944–50. doi: 10.1021/ac1001959.

[48] Ye C, Zhang F, Tan X, Sun H, Dai W, Yang K, et al. A dense graphene monolith with poloxamer prefunctionalization enabling aqueous redispersion to obtain solubilized graphene sheets. *Chin Chem Lett*. 2020;31(9):2507–11.

[49] Zhu Y, Tian Q, Li X, Wu L, Yu A, Lai G, et al. A double-deck structure of reduced graphene oxide modified porous Ti<sub>3</sub>C<sub>2</sub>Tx electrode towards ultrasensitive and simultaneous detection of dopamine and uric acid. *Biosensors*. 2021;11(11):462.

[50] Fu L, Wang A, Su W, Zheng Y, Liu Z. A rapid electrochemical sensor fabricated using silver ions and graphene oxide. *Ionics*. 2018;24:2821–7.

[51] Fu L, Lai G, Zhu D, Jia B, Malherbe F, Yu A. Advanced catalytic and electrocatalytic performances of polydopamine-functionalized reduced graphene oxide-palladium nanocomposites. *ChemCatChem*. 2016;8(18):2975–80.

[52] Huang J-Y, Zhao L, Lei W, Wen W, Wang Y-J, Bao T, et al. A high-sensitivity electrochemical aptasensor of carcinoembryonic antigen based on graphene quantum dots-ionic liquid-nafion nanomatrix and DNAzyme-assisted signal amplification strategy. *Biosens Bioelectron*. 2018;99:28–33. doi: 10.1016/j.bios.2017.07.036.

[53] Mollarasouli F, Kurbanoglu S, Ozkan SA. The role of electrochemical immunosensors in clinical analysis. *Biosensors*. 2019;9(3):86.

[54] Feng S, Yan M, Xue Y, Huang J, Yang X. Electrochemical immuno-sensor for cardiac troponin I detection based on covalent organic framework and enzyme-catalyzed signal amplification. *Anal Chem*. 2021;93(40):13572–9.

[55] Yang H, Bao J, Huo D, Zeng Y, Wang X, Samalo M, et al. Au doped poly-thionine and poly-m-Cresol purple: Synthesis and their application in simultaneously electrochemical detection of two lung cancer markers CEA and CYFRA21-1. *Talanta*. 2021;224:121816. doi: 10.1016/j.talanta.2020.121816.

[56] Oh C, Park B, Li C, Maldarelli C, Schaefer JL, Datta-Chaudhuri T, et al. Electrochemical immunoassay of interleukin-6 in human cerebrospinal fluid and human serum as an early biomarker for traumatic brain injury. *ACS Meas Sci Au*. 2021;1(2):65–73. doi: 10.1021/acsmmeasci.1c00013.

[57] Karimi-Maleh H, Darabi R, Baghayeri M, Karimi F, Fu L, Rouhi J, et al. Recent developments in carbon nanomaterials-based electrochemical sensors for methyl parathion detection. *J Food Meas Charact*. 2023;17(5):5371–89.

[58] Shi P, Xie R, Wang P, Lei Y, Chen B, Li S, et al. Non-covalent modification of glassy carbon electrode with isoorientin and application to alpha-fetoprotein detection by fabricating an immunoassay. *Sens Actuators B: Chem*. 2020;305:127494.

[59] Zhou Y, Fang Y, Ramasamy RP. Non-covalent functionalization of carbon nanotubes for electrochemical biosensor development. *Sensors*. 2019;19(2):392.

[60] Weng X-H, Xu X-W, Huang P-F, Liu Z-J, Liu A-L, Lin Z-Y, et al. A multiple signal amplification electrochemical biosensors based on target DNA recycling for detection of the EGFR mutation status in lung cancer patients. *J Electroanal Chem*. 2019;853:113555. doi: 10.1016/j.jelechem.2019.113555.

[61] Chen D, Luo X, Xi F. Probe-integrated electrochemical immunoassay based on electrostatic nanocage array for reagentless and sensitive detection of tumor biomarker. *Front Chem*. 2023;11:1121450.

[62] Karimi-Maleh H, Ghalkhani M, Saberi Dehkordi Z, Mohsenpour Tehran M, Singh J, Wen Y, et al. MOF-enabled pesticides as developing approach for sustainable agriculture and reducing environmental hazards. *J Ind Eng Chem*. 2023;129:105–23. doi: 10.1016/j.jiec.2023.08.044.

[63] Lütfi Yola M, Atar N, Özcan N. A novel electrochemical lung cancer biomarker cytokeratin 19 fragment antigen 21-1 immunoassay based on  $\text{Si}_3\text{N}_4/\text{MoS}_2$  incorporated MWCNTs and core-shell type magnetic nanoparticles. *Nanoscale*. 2021;13(8):4660–9. doi: 10.1039/D1NR00244A.

[64] Khalilzadeh B, Shadjou N, Eskandani M, Nozad Charoudeh H, Omidi Y, Rashidi M-R. A reliable self-assembled peptide based electrochemical biosensor for detection of caspase 3 activity and apoptosis. *RSC Adv*. 2015;5(72):58316–26. doi: 10.1039/C5RA08561F.

[65] Kim D-M, Noh H-B, Park DS, Ryu S-H, Koo JS, Shim Y-B. Immunosensors for detection of Annexin II and MUC5AC for early diagnosis of lung cancer. *Biosens Bioelectron*. 2009;25(2):456–62. doi: 10.1016/j.bios.2009.08.007.

[66] Cheng Y, Yuan R, Chai Y, Niu H, Cao Y, Liu H, et al. Highly sensitive luminol electrochemiluminescence immunoassay based on  $\text{ZnO}$  nanoparticles and glucose oxidase decorated graphene for cancer biomarker detection. *Anal Chim Acta*. 2012;745:137–42. doi: 10.1016/j.aca.2012.08.010.

[67] Li Y, Zhang Y, Li F, Feng J, Li M, Chen L, et al. Ultrasensitive electrochemical immunoassay for quantitative detection of SCCA using  $\text{Co}_3\text{O}_4@\text{CeO}_2\text{-Au}@\text{Pt}$  nanocomposite as enzyme-mimetic labels. *Biosens Bioelectron*. 2017;92:33–9. doi: 10.1016/j.bios.2017.01.065.

[68] Idris AO, Mabuba N, Arotiba OA. An Exfoliated Graphite-Based Electrochemical Immunoassay on a Dendrimer/Carbon Nanodot Platform for the Detection of Carcinoembryonic Antigen Cancer Biomarker. *Biosensors*. 2019;9(1):39. doi: 10.3390/bios9010039.

[69] Liu S, Su W, Li Z, Ding X. Electrochemical detection of lung cancer specific microRNAs using 3D DNA origami nanostructures. *Biosens Bioelectron*. 2015;71:57–61. doi: 10.1016/j.bios.2015.04.006.

[70] Wang Q, Xin H, Wang Z. Label-free immunoassay based on poly-aniline-loaded MXene and gold-decorated  $\beta$ -cyclodextrin for efficient detection of carcinoembryonic antigen. *Biosensors*. 2022;12(8):657. doi: 10.3390/bios12080657.

[71] Gan N, Jia L, Zheng L. A sandwich electrochemical immunoassay using magnetic DNA nanoprobes for carcinoembryonic antigen. *Int J Mol Sci*. 2011;12(11):7410–23. doi: 10.3390/ijms12117410.

[72] Wang Y, Wang H, Bai Y, Zhao G, Zhang N, Zhang Y, et al.  $\text{MoS}_2@\text{Au}$  as label for sensitive sandwich-type immunoassay of neuron-specific enolase. *Chemosensors*. 2023;11(6):349. doi: 10.3390/chemosensors11060349.

[73] Karaman C, Böülübaşı ÖS, Yola BB, Karaman O, Atar N, Yola ML. Electrochemical neuron-specific enolase (NSE) immunoassay based on  $\text{CoFe}_2\text{O}_4@\text{Ag}$  nanocomposite and  $\text{AuNPs@MoS}_2/\text{rGO}$ . *Anal Chim Acta*. 2022;1200:339609. doi: 10.1016/j.aca.2022.339609.

[74] Han J, Zhuo Y, Chai Y-Q, Yuan Y-L, Yuan R. Novel electrochemical catalysis as signal amplified strategy for label-free detection of neuron-specific enolase. *Biosens Bioelectron*. 2012;31(1):399–405. doi: 10.1016/j.bios.2011.10.055.

[75] Kumar S, Panwar S, Kumar S, Augustine S, Malhotra BD. Biofunctionalized nanostructured yttria modified non-invasive impedimetric biosensor for efficient detection of oral cancer. *Nanomaterials*. 2019;9(9):1190. doi: 10.3390/nano9091190.

[76] Aydin EB, Aydin M, Sezgitürk MK. Novel electrochemical biosensing platform based on conductive multilayer for sensitive and selective detection of CYFRA 21-1. *Sens Actuators B: Chem*. 2023;378:133208. doi: 10.1016/j.snb.2022.133208.

[77] Lu J, Hao L, Yang F, Liu Y, Yang H, Yan S. Ultrasensitive electrochemical detection of CYFRA 21-1 via in-situ initiated ROP signal amplification strategy. *Anal Chim Acta*. 2021;1180:33889. doi: 10.1016/j.aca.2021.33889.

[78] Wei Z, Cai X, Zhang J, Fan J, Xu J, Xu L. High sensitive immunoelectrochemical measurement of lung cancer tumor marker ProGRP based on  $\text{TiO}_2\text{-Au}$  nanocomposite. *Molecules*. 2019;24(4):656. doi: 10.3390/molecules24040656.

[79] Amouzadeh Tabrizi M, Shamsipur M, Farzin L. A high sensitive electrochemical aptasensor for the determination of VEGF165 in serum of lung cancer patient. *Biosens Bioelectron*. 2015;74:764–9. doi: 10.1016/j.bios.2015.07.032.

[80] Liu S, Su W, Li Y, Zhang L, Ding X. Manufacturing of an electrochemical biosensing platform based on hybrid DNA hydrogel: Taking lung cancer-specific miR-21 as an example. *Biosens Bioelectron*. 2018;103:1–5. doi: 10.1016/j.bios.2017.12.021.

[81] Xu X-W, Weng X-H, Wang C-L, Lin W-W, Liu A-L, Chen W, et al. Detection EGFR exon 19 status of lung cancer patients by DNA electrochemical biosensor. *Biosens Bioelectron*. 2016;80:411–7. doi: 10.1016/j.bios.2016.02.009.